

**THE LIMITING SHAPES OF GRAVITATIONALLY BOUND, ROTATING SAND PILES.** D.A. Minton, Lunar and Planetary Laboratory, The University of Arizona, 1629 E. University Blvd. Tucson AZ 85721. daminton@lpl.arizona.edu.

**Introduction:** What would a self-gravitating, rotating sand pile look like if every slope on the surface was at the angle of repose? Many asteroids are likely gravitationally bound aggregates of collisional fragments [1]. Gravitational aggregates are often called “strengthless,” however internal friction and interlocking between particles can maintain topography that is out of hydrostatic equilibrium. One can observe that loose piles of aggregated particles, like sand, have slopes that are maintained at what is called the *angle of repose*,  $\phi$ , where typically  $20^\circ \lesssim \phi \lesssim 30^\circ$  with respect to horizontal [e.g., 2, 3]. The purpose of this study is to explore the topographic limits of a hypothetical asteroid composed entirely of loose sand. What would a self-gravitating, rotating sand pile look like if every slope on the surface was at the angle of repose?

Other attempts have been made to establish the shapes of angle of repose-limited rubble pile asteroids using a variety of techniques [4–9]. Here I calculate uniform density, three-dimensional objects for which the surface at every point is at an angle  $\phi$  relative to the local horizontal as defined by the sum of the gravitational and centripetal acceleration vectors at that point. This can be expressed by the following equation:

$$\hat{\mathbf{N}} \cdot \hat{\mathbf{g}}_{eff} + \cos \phi = 0, \quad (1)$$

where  $\hat{\mathbf{N}}$  is the unit normal vector at a point on the surface, and  $\hat{\mathbf{g}}_{eff}$  is the effective gravitational unit vector at the same point, which includes contributions from the gravitational and the centripetal acceleration vectors. If  $\phi = 0$ , then Eq. (1) describes a fluid in hydrostatic equilibrium, and analytical solutions for isolated bodies were found by Maclaurin and Jacobi [e.g., 10]. For the case where  $\phi \neq 0$  everywhere, no closed-form analytical solutions are known. To solve this problem I have developed an iterative numerical technique that has been implemented in a code called *Sandyroid*.

**Non-rotating solutions:** The term “angle of repose” refers to the magnitude of the slope, but the sign of the slope along a profile can abruptly change at “cusps.” Cusps can be either point or line cusps and can have a “positive” or a “negative” orientation. Because the number and configuration of cusps is unconstrained, only a small subset of possible solutions were explored. The search for solution shapes was limited to angles of repose in the range of  $20^\circ \leq \phi \leq 30^\circ$  and to five different cusp configurations.

Three cusp configurations yielded solutions, which have been named “Donut,” “Top,” and “Hourglass.” Solutions were found for Donut with  $\phi \lesssim 21^\circ$ , for Top with  $\phi \lesssim 22^\circ$ , and for Hourglass with  $\phi \lesssim 28^\circ$ . Figure 1 shows non-rotating solution shapes for the three configurations considered here. The surface angles of the final solution meshes are within approximately  $\pm 1^\circ$  of the target surface angles.

**Rotating solutions:** *Sandyroid* is able to calculate solution shapes with rotation about the x-, y-, or z-axes. Only solutions that have rotation about a stable axis are considered here.

The first rotational case considered for which solutions

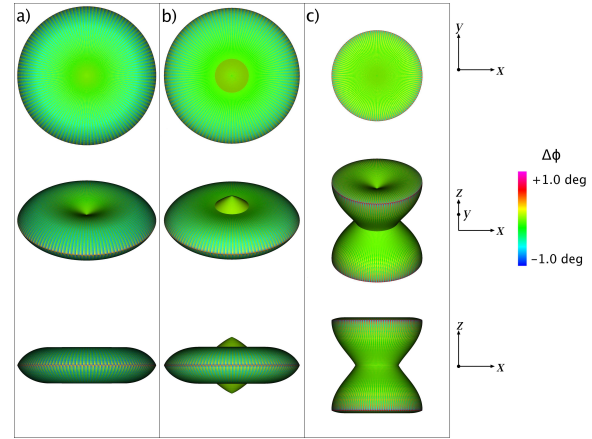


Figure 1: Highest-angle, non-rotating constant surface angle solutions for a) Donut ( $\phi = 21^\circ$ ), b) Top ( $\phi = 22^\circ$ ), and c) Hourglass ( $\phi = 28^\circ$ ). Three different orientations are shown for each of the three configurations, with the top row corresponding to a view of the top of the objects, the bottom row corresponding to a view of the front of the objects, and the middle row corresponding to an intermediate view. Colors represent the deviation of the surface angle of the facets from the target surface angle, computed using *Polygrav*. Each surface mesh contains 56400 triangular facets.

were found is the “Oblate Donut,” which has the same cusp configuration as Donut, but with rotation about the z-axis. By varying the rotation rate as well as the angle of repose, a direct comparison can be made with Holsapple (2001) [5], who explored equilibrium configurations of rubble piles using an internal yield stress criterion, rather than the purely geometrical criterion chosen for this study. The two ratios of object dimensions are given as:

$$\begin{aligned} \alpha &= c/a, \\ \beta &= b/a, \end{aligned} \quad (2)$$

where the dimensions are defined to be the maximum extent of the object along a principal axis, and  $a \geq b \geq c$ .

The results of several Oblate Donut solution shapes determined by *Sandyroid* are compared to the equilibrium configurations determined by Holsapple (2001) for oblate spheroids in Figure 2. Note that *Sandyroid* is capable of reproducing a portion of the classic Maclaurin spheroid curve when given  $\phi = 0^\circ$ . For  $\phi > 0^\circ$  *Sandyroid* produces a lower value of  $\alpha$  for any given rotation rate than the limit derived by Holsapple for his oblate spheroid solutions.

Sets of z-axis rotating solutions to the Top configuration, called “Oblate Top” were also found. For the Hourglass configuration, the body must be rotated about either its x- or y-axis to achieve stable principal axis rotation for a wide range of

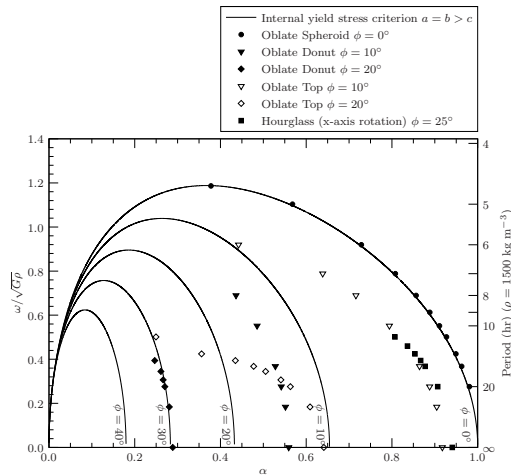


Figure 2: Relationship between rotation rate and body aspect ratio. The points represent *Sandyroid* solutions for several configurations, angles of repose, and rotation rates. Also plotted are curves of the required angle of internal friction determined by Holsapple (2001) [5] (only the  $\sigma_x = \sigma_y < \sigma_z$  branch is shown). The curve for  $\phi = 0^\circ$  is the classic Maclaurin spheroid, which is partially reproduced by *Sandyroid*. For each configuration shown here, the most rapidly rotating solution that *Sandyroid* was able to calculate is plotted. Profile generation fails either when a singularity develops in the seed body or the centripetal acceleration becomes greater than the gravitational acceleration at some point along the profile.

rotation rates.

*Sandyroid* was unable to converge on solutions for either Donut or Top with x- or y-axis rotation. Attempts were also made to produce Jacobi ellipsoids using *Sandyroid* by supplying it with highly elongated initial seed shapes and setting  $\phi = 0^\circ$ , but these attempts were not successful. The inability of *Sandyroid* to produce Jacobi ellipsoids may indicate that some solutions to Eq. (1) are not numerically stable in *Sandyroid*. As Figure 1 demonstrates, the shapes that *Sandyroid* was capable of producing are objects whose entire surfaces have slopes that are constant within  $\pm 1^\circ$ .

**Comparisons between angle of repose-limited bodies and observed small bodies:** Unlike fluid bodies, gravitational aggregates can maintain a range of equilibrium shapes. The solution shapes produced by *Sandyroid* represent limiting cases. Because the angle of repose-limited solutions described here are idealized mathematical constructs, some caution is warranted when comparisons are made to the shapes of natural bodies. Nevertheless, some intriguing similarities can be found between the shapes presented here and real small bodies that have been observed.

Radar imaging of the near-Earth asteroid 1999 KW4 revealed that it has an equatorial ridge that is similar to the positive equatorial cusps found on both Donut and Top [11]. The Saturnian satellite Atlas shows a striking similarity to both Donut and Atlas, especially in the equatorial region, as shown

in Figure 3. It has been proposed that the equatorial region of Atlas is composed of ring material that preferentially falls onto the satellite's equator [12–14]. If this is the case, then the shape of Atlas may indicate that the loose ring material may be at or near the angle of repose. The Hourglass bodies somewhat resemble contact binaries.

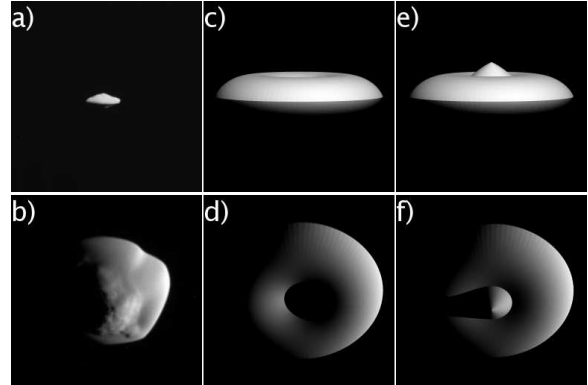


Figure 3: a),b) Two views of the Saturnian moon Atlas as imaged by the Cassini Imagine Science Subsystem (ISS) narrow angle camera. c),d) Views of Donut with no rotation and  $\phi = 21^\circ$  with similar orientation and lighting as the Atlas images. e),f) Views of Top with no rotation and  $\phi = 22^\circ$  with similar orientation and lighting as the Atlas images. Atlas images courtesy NASA/JPL-Caltech.

**Summary:** The shapes produced by *Sandyroid* are idealized mathematical constructs that represent limiting cases. These shapes are not unique, and as the failure of *Sandyroid* to produce Jacobi ellipsoids demonstrates, there may be other solution shapes that it is incapable of producing. Nevertheless, the shapes that are produced by *Sandyroid* are robust in the sense that the discretized solution objects have surfaces that are computed to be at a constant angle relative to their local gravitational vector, within the limits of mesh resolution.

#### References:

- [1] Richardson D.C. et al. (2002) in *Asteroids III*, edited by W.F. Bottke Jr., A. Cellino, P. Paolicchi and R.P. Binzel, 501–515, Univ. of Arizona Press, Tucson.
- [2] Bretz M. et al. (1992) *Phys. Rev. Lett.*, 69, 2431–2434.
- [3] Buchholtz V. and Pöschel T. (1994) *Physica A Statistical Mechanics and its Applications*, 202, 390–401.
- [4] Withers P. (2000) *Lunar and Planet. Sci.*, XXXI, 1270 (abstract).
- [5] Holsapple K.A. (2001) *Icarus*, 154, 432–448.
- [6] Holsapple K.A. (2004) *Icarus*, 172, 272–303.
- [7] Holsapple K.A. and Michel P. (2006) *Icarus*, 183, 331–348.
- [8] Holsapple K.A. (2007) *Icarus*, 187, 500–509.
- [9] Richardson D.C. et al. (2005) *Icarus*, 173, 349–361.
- [10] Chandrasekhar S. (1969) *Ellipsoidal figures of equilibrium*, The Silliman Foundation Lectures, New Haven: Yale University Press.
- [11] Ostro S.J. and 15 colleagues (2006) *Science*, 314, 1276–1280.
- [12] Brahic A. et al. (2006) *Bull. Am. Astron. Soc.*, 38, 629 (abstract).
- [13] Porco C. et al. (2006) *Eos (Fall Suppl.)*, 87, 52.
- [14] Thomas P.C. et al. (2007) *Bull. Am. Astron. Soc.*, 39, (abstract).